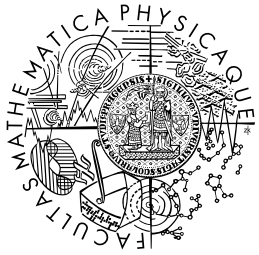

FACULTY
OF MATHEMATICS
AND PHYSICS
Charles University

BACHELOR THESIS

Hedvika Gedeonová

Time-Dependent Solution of the Generalized Fano Model

Institute of Theoretical Physics

Supervisor of the bachelor thesis: RNDr. Přemysl Kolorenč, Ph.D.
Study programme: Physics
Study branch: Theoretical Physics

Prague 2017

I declare that I carried out this bachelor thesis independently, and only with the cited sources, literature and other professional sources.

I understand that my work relates to the rights and obligations under the Act No. 121/2000 Sb., the Copyright Act, as amended, in particular the fact that the Charles University has the right to conclude a license agreement on the use of this work as a school work pursuant to Section 60 subsection 1 of the Copyright Act.

In Prague 26.6. 2017

Title: Time-Dependent Solution of the Generalized Fano Model

Author: Hedvika Gedeonová

Institute: Institute of Theoretical Physics

Supervisor: RNDr. Přemysl Kolorenč, Ph.D., Institute of Theoretical Physics

Abstract:
In this thesis, the time evolution of Fano model, describing a discrete state embedded in a continuum of states with constant coupling, and generalized version of Fano model for an energy dependent coupling are investigated. For the time evolution of the generalized system, numerical simulation (Gaussian quadrature and numerical integration of a system of differential equations) is used. The system behaves as Fano model predicts when energy-dependent coupling tends to a constant one, and the system exponentially decays into the continuum. For a strongly energy-dependent coupling, the system oscillates between the initial discrete state and the continuum. The thesis provides numerically evaluated time evolution for different parameters of the coupling, brief interpretation of probability oscillation phenomenon and study of the transition between oscillatory and non-oscillatory mode.

Keywords: Resonance scattering, Generalized Fano model, Numerically simulated decay

I would like to thank my supervisor RNDr. Přemysl Kolorenč, Ph.D. for all valuable advice, inspirational ideas and patient guidance throughout the whole process of writing this thesis.

My gratitude also belongs to Hodňoulinký tatíneček, Trpaslík and both Tigers for unconditional love and overall support and especially to Kozlíček for his never-ending love and his unique warm hugs.

Contents

Introduction

Variety of physical processes in quantum mechanics can be described as an interaction of the so called discrete state with a continuum. Resonant scattering can serve as a most typical example. One of simple models, introduced by Ugo Fano, assumes the decay of the discrete state into a continuum of states, driven by a constant coupling (i.e., independent of the energy of the continuum states). In such case, the decay is exponential.

We will generalize Fano model in order to describe similar system, but this time with an energy-dependent coupling, which is much closer to many physical processes seen in nature.

In the first chapter of this thesis, we shall discus Fano model in more detail and we will introduce natural way of dealing with it. By discretization of the continuum of states and finding eigenstates of the resulting Hamiltonian, we will be able to find the exact time evolution of the system. We than generalize Fano model to energy-dependent coupling and introduce simple way to numerically determine time evolution for this generalized system.

In the second chapter, we will discus some aspects of the time evolution (probability of finding the system in the initial discrete state), mainly the dependence on different parameters of the coupling. We shall see that for particular parameters the probability exponentially decrease, whilst for others the probability oscillates. We shall study the oscillatory and the non-oscillatory mode, as well as the transition between them.

In the whole thesis, we use atomic units with $\hbar = e = m_e = 1$.

1. Theoretical Background

1.1 Fano Model

A simple model, first introduced by U. Fano, describes decay of a discrete state into a continuum of states. The model considers a Hamiltonian $\mathbb{H}_0$, which has as eigenstates the continuum of states $|E\rangle$ and the discrete state $|\varphi\rangle$, coupled to the continuum by a constant (i.e., independent of energy of the $|E\rangle$) coupling Hamiltonian V.

We shall assume that V is not explicitly time-dependent, has zero diagonal elements, and that V cannot couple two states of the continuum:

$$\begin{cases} \langle\varphi|V|\varphi\rangle = 0, \\ \langle E|V|E\rangle = 0, \\ \langle E|V|E'\rangle = 0. \end{cases} \tag{1.1}$$

The only non-zero element is therefore $\langle E|V|\varphi\rangle$, which is responsible for the decay of $|\varphi\rangle$. In the basis of $|\varphi\rangle$ and the continuum eigenstates $|E\rangle$ of $\mathbb{H}_0$, the full Hamiltonian matrix is

$$\mathbb{H} = \left(\begin{array}{c|ccc} E_\varphi & & V & \\ \hline & \ddots & & 0 \\ V^* & & E & \\ & 0 & & \ddots \end{array}\right). \tag{1.2}$$

1.1.1 Discretization of the Continuum

In order to analyse time evolution of such a system analytically, we replace the states of continuum $|E\rangle$ by discretized spectrum of states $|k\rangle$ spaced by δ in energy. From this we can simply obtain physical results when δ tends to zero.

We will require similar condition for the new quasi-continuum:

- The discretized continuum extends over interval $(-\infty, \infty)$ with equidistant levels spaced by δ. Therefore

  $$\langle k|\mathbb{H}_0|k\rangle = E_k = k\delta, \qquad k \in \mathbb{Z}. \tag{1.3}$$

  For what follows, we set origin of the energy axis at the energy of the discrete state, i.e., $E_\varphi = \langle\varphi|\mathbb{H}_0|\varphi\rangle = 0$.

- For the coupling, we assume all the matrix elements of V between the level $|\varphi\rangle$ and $|k\rangle$ are equal and real:

  $$\nu = \langle k|V|\varphi\rangle = \langle\varphi|V|k\rangle \tag{1.4}$$

- All the other matrix elements of V are zero:

  $$\langle\varphi|V|\varphi\rangle = \langle k|V|k'\rangle = 0 \tag{1.5}$$

If we denote Γ the transition probability an ρ the density of final states (the quasi-continuum) we can write Fermi's golden rule in a form

$$\Gamma = 2\pi|\nu|^2\rho(E_\varphi), \tag{1.6}$$

where in our case $\nu = \langle\varphi|V|k\rangle$. As $\rho = 1/\delta$, we can rewrite previous equation to

$$\Gamma = \frac{2\pi|\nu|^2}{\delta} \tag{1.7}$$

and as Γ must remain constant even when $\delta \to 0$, one can derive

$$\frac{\nu^2}{\delta} = \frac{\Gamma}{2\pi}. \tag{1.8}$$

1.1.2 Stationary States of the System

Let now have the full Hamiltonian $\mathbb{H} = \mathbb{H}_0 + V$ with E_μ as eigenvalue and $|\Psi_\mu\rangle$ as eigenstate. If we project Schrödinger equation

$$\mathbb{H}|\Psi_\mu\rangle = E_\mu|\Psi_\mu\rangle \tag{1.9}$$

onto $\langle k|$ and $\langle\varphi|$, using relations $E_\varphi = 0$, (1.3), (1.4), and (1.5), we obtain respectively

$$E_k\langle k|\Psi_\mu\rangle + \nu\langle\varphi|\Psi_\mu\rangle = E_\mu\langle k|\Psi_\mu\rangle, \tag{1.10a}$$

$$\sum_k \nu\langle k|\Psi_\mu\rangle = E_\mu\langle\varphi|\Psi_\mu\rangle. \tag{1.10b}$$

which together yield eigenvalue equation

$$\sum_k \frac{\nu^2}{E_\mu - E_k} = \frac{1}{\delta}\sum_k \frac{\nu^2}{\frac{E_\mu}{\delta} - k} = E_\mu. \tag{1.11}$$

It can be shown that

$$\sum_k (z-k)^{-1} = \frac{\pi}{\tan(\pi z)}, \tag{1.12a}$$

$$\sum_k (z-k)^{-2} = \frac{\pi^2}{\sin^2(\pi z)}, \tag{1.12b}$$

which used for (1.11) together with (1.8) gives

$$\frac{E_\mu}{\delta} = m + \frac{\arctan\left(\frac{\Gamma}{2E_\mu}\right)}{\pi}, \tag{1.13}$$

where m is any integer. We can solve this resulting eigenvalue equation numerically.

1.1.3 Decay of the Discrete Level

In this section we will study behaviour of the system initially prepared in the state corresponding to the discrete level $|\varphi\rangle$. If we add the normalization condition

$$\sum_k |\langle k|\Psi_\mu\rangle|^2 + |\langle\varphi|\Psi_\mu\rangle|^2 = 1, \tag{1.14}$$

to (1.10), we obtain

$$\langle\varphi|\Psi_\mu\rangle = \frac{1}{\left[1+\sum_{k'}\left(\frac{\nu}{E_\mu - E_{k'}}\right)^2\right]^{1/2}}, \tag{1.15a}$$

$$\langle k|\Psi_\mu\rangle = \frac{\frac{\nu}{E_\mu - E_k}}{\left[1+\sum_{k'}\left(\frac{\nu}{E_\mu - E_{k'}}\right)^2\right]^{1/2}}, \tag{1.15b}$$

and using (1.12b), (1.11), and (1.8) we get

$$\langle\varphi|\Psi_\mu\rangle = \frac{\nu}{\left[\nu^2 + \left(\frac{\Gamma}{2}\right)^2 + E_\mu^2\right]^{1/2}}. \tag{1.16}$$

Now we can calculate the probability of finding the system still in the discrete state $|\varphi\rangle$ after time t, if we expand $|\varphi\rangle$ into the basis of eigenstates $|\Psi_\mu\rangle$ of Hamiltonian $\mathbb{H} = \mathbb{H}_0 + V$ and using (1.16):

$$|\varphi(0)\rangle = \sum_\mu \frac{\nu}{\left[\nu^2 + \left(\frac{\Gamma}{2}\right)^2 + E_\mu^2\right]^{1/2}}|\Psi_\mu\rangle. \tag{1.17}$$

Therefore, the state will evolve in time as

$$|\varphi(t)\rangle = \sum_\mu \frac{\nu}{\left[\nu^2 + \left(\frac{\Gamma}{2}\right)^2 + E_\mu^2\right]^{1/2}} e^{-iE_\mu t}|\Psi_\mu\rangle, \tag{1.18}$$

which yields the probability of finding the system in $|\varphi\rangle$ equal to

$$\langle\varphi|\varphi(t)\rangle = \delta\sum_\mu \frac{\frac{\Gamma}{2\pi}}{\frac{\Gamma\delta}{2\pi} + \left(\frac{\Gamma}{2}\right)^2 + E_\mu^2} e^{-iE_\mu t}, \tag{1.19}$$

where we used formula (1.8) for ν. As the δ tends to 0, E_μ tends to continuum and the sum becomes an integral, so we get

$$\langle\varphi|\varphi(t)\rangle = \int_{-\infty}^{\infty} \frac{\Gamma}{2\pi}\frac{e^{-iEt}}{\left(\frac{\Gamma}{2}\right)^2 + E^2}\mathrm{d}E = e^{-\frac{\Gamma|t|}{2}}, \tag{1.20}$$

from which the probability is

$$|\langle\varphi|\varphi(t)\rangle|^2 = e^{-\Gamma|t|}. \tag{1.21}$$

So Γ^{-1} is the decay constant of our system.
For more details about Fano model, see [1] and [2].

1.2 Generalization for Energy-Dependent Coupling

As we have seen above, Fano model is restricted to constant coupling (see (1.4)). We would like to find more general description, allowing as to solve more realistic problem

$$\nu(E) = \langle k|V|\varphi\rangle, \tag{1.22}$$

where ν is now a function of energy of the continuum E. For that we need to relax some of our assumptions. The Hamiltonian (1.2) still remains with the coupling in a form

$$\langle\varphi|\mathbb{H}|E\rangle = V = \alpha e^{-\beta E^2}, \tag{1.23}$$

where $|\varphi\rangle$ is the initial discrete state (i.e., at time $t = 0$), E is energy of state of the continuum to which is $|\varphi\rangle$ coupled, and α, $\beta \in \mathbb{R}$ are parameters.

We require normalization:

- $\langle\varphi|\varphi\rangle = 1$
- $\langle\varphi|E\rangle = 0$
- $\langle E|E'\rangle = \delta(E - E')$

Time evolution of any time-dependent wave function $|\Psi(t)\rangle$ is determined by Schrödinger equation

$$i\frac{\mathrm{d}|\Psi\rangle}{\mathrm{d}t} = \mathbb{H}|\Psi\rangle, \tag{1.24}$$

and as $|\Psi(t)\rangle$ can be expressed as a linear combination of $|\varphi\rangle$ and $|E\rangle$

$$|\Psi(t)\rangle = a(t)|\varphi\rangle + \int_{-\infty}^{\infty} b(t,\epsilon)|E\rangle\mathrm{d}\epsilon. \tag{1.25}$$

we can rewrite (1.24) to

$$i\frac{\mathrm{d}|\Psi\rangle}{\mathrm{d}t} = i\frac{\mathrm{d}a(t)}{\mathrm{d}t}|\varphi\rangle + i\int_{-\infty}^{\infty}\frac{\mathrm{d}b(t,E)}{\mathrm{d}t}|E\rangle\mathrm{d}E = a(t)\mathbb{H}|\varphi\rangle + \int_{-\infty}^{\infty} b(t,E)\mathbb{H}|E\rangle\mathrm{d}E, \tag{1.26}$$

Now we project (1.26) onto $\langle\varphi|$ and $\langle E|$, which gives us respectively ($E_\varphi = 0$)

$$i\frac{\mathrm{d}a(t)}{\mathrm{d}t} = \int_{-\infty}^{\infty} b(t,E)V(E)\mathrm{d}E, \tag{1.27a}$$

$$i\frac{\mathrm{d}b(t,E)}{\mathrm{d}t} = a(t)V^* + b(t,E)E, \tag{1.27b}$$

which is a set of differential equations for unknown coefficients $a(t)$ and $b(t,E)$. We add an initial condition $|\Psi(t=0)\rangle = |\varphi\rangle$ ($\Leftrightarrow a(0) = 1$, $b(0,\epsilon) = 0$).

Our goal is to calculate the probability of finding $|\Psi(t)\rangle$ in the state $|\varphi\rangle$, that means

$$|\langle\varphi|\Psi(t)\rangle|^2 = |a(t)|^2 \tag{1.28}$$

for which we need to know $a(t)$, i.e., to solve (1.27). For that we first discretize continuum $|E\rangle$ to $|k\rangle$ as described in previous section. The discretized continuum can be then treated numerically and (1.27) can be solved with numerical methods, as we are not able to solve it analytically.

1.3 Oscillations in Two and Three Level System

We will see later that in the generalized Fano model, the probability (1.28) starts to oscillate for specific value α and β (see equation (1.23)). To better understand this phenomenon, we will examine two simpler models - two and three level systems.

Consider first a system of two levels that are not eigenstates of the Hamiltonian. Any state $|\Psi\rangle$ can be represented as a linear combination of these two states:

$$|\Psi\rangle = c_1 \begin{pmatrix} 1 \\ 0 \end{pmatrix} + c_2 \begin{pmatrix} 0 \\ 1 \end{pmatrix} \equiv c_1|1\rangle + c_2|2\rangle, \qquad |c_1|^2 + |c_2|^2 = 1. \tag{1.29}$$

The probability of finding a state initially prepared as $|1\rangle$ in $|2\rangle$ oscillates with characteristic frequency Ω, also known as Rabi frequency.

Now, if we want to find this frequency as a function of matrix elements of given 2x2 Hamiltonian $\mathbb{H}$, we must first rewrite $\mathbb{H}$ in terms of Pauli matrices σ:

$$\mathbb{H} = a_0\sigma_0 + a_1\sigma_1 + a_2\sigma_2 + a_3\sigma_3. \tag{1.30}$$

Denoting E_1, E_2 the two eigenvalues and $|E_1\rangle$, $|E_2\rangle$, respectively, the two eigenstates of $\mathbb{H}$ (in the basis of $|1\rangle$, $|2\rangle$), we can write

$$E_1 = a_0 + \sqrt{a_1^2 + a_2^2 + a_3^2}, \tag{1.31a}$$

$$E_2 = a_0 - \sqrt{a_1^2 + a_2^2 + a_3^2}, \tag{1.31b}$$

$$|E_1\rangle = \begin{pmatrix} \cos\left(\frac{\theta}{2}\right) \\ e^{-i\phi}\sin\left(\frac{\theta}{2}\right) \end{pmatrix}, \tag{1.31c}$$

$$|E_2\rangle = \begin{pmatrix} -e^{i\phi}\sin\left(\frac{\theta}{2}\right) \\ \cos\left(\frac{\theta}{2}\right) \end{pmatrix}, \tag{1.31d}$$

where $e^{-i\phi}$ is an arbitrary phase and

$$\theta = \arcsin\left(\sqrt{\frac{a_1^2 + a_2^2}{a_1^2 + a_2^2 + a_3^2}}\right) = \arccos\left(\frac{a_3}{\sqrt{a_1^2 + a_2^2 + a_3^2}}\right). \tag{1.32}$$

Let the system initial state be $|1\rangle$, that is,

$$|\Psi(0)\rangle = |1\rangle = \cos\left(\frac{\theta}{2}\right)|E_1\rangle - e^{-i\phi}\sin\left(\frac{\theta}{2}\right)|E_2\rangle. \tag{1.33}$$

Then

$$|\Psi(t)\rangle = e^{-itE_1}\cos\left(\frac{\theta}{2}\right)|E_1\rangle - e^{-i\phi}e^{-itE_2}\sin\left(\frac{\theta}{2}\right)|E_2\rangle, \tag{1.34}$$

and the probability of finding $|\Psi(t)\rangle$ in $|2\rangle$ is

$$|\langle 2|\Psi(t)\rangle|^2 = \left| \left(e^{i\phi} \sin\left(\frac{\theta}{2}\right) \langle E_1| + \cos\left(\frac{\theta}{2}\right) \langle E_2| \right) |\Psi(t)\rangle \right|^2$$
$$= \frac{1}{2}\sin^2\theta\,(1-\cos\left(t(E_1-E_2)\right)) = \frac{(a_1^2+a_2^2)^2}{a_1^2+a_2^2+a_3^2}\sin^2\left(t\frac{(E_1-E_2)}{2}\right), \quad (1.35)$$

which is known as Rabi formula [3].

The probability oscillates in time with characteristic frequency

$$\Omega = E_1 - E_2 = 2\sqrt{a_1^2+a_2^2+a_3^2}. \quad (1.36)$$

Similarly, it can be shown that the probability of finding system in $|1\rangle$ is also oscillatory with the same frequency Ω. If this phenomenon is driven by external field, it is called Rabi oscillations [3].

As we will be working with Hamiltonians of a form (V, ϵ assumed real)

$$\mathbb{H}^{(2)} = \begin{pmatrix} 0 & V \\ V & \epsilon \end{pmatrix}, \quad (1.37)$$

and

$$\mathbb{H}^{(3)} = \begin{pmatrix} -\epsilon & V & 0 \\ V & 0 & V \\ 0 & V & \epsilon \end{pmatrix}, \quad (1.38)$$

it is convenient to find Rabi frequency for these two special cases. Our two states will be

$$|1^{(2)}\rangle \equiv \begin{pmatrix} 1 \\ 0 \end{pmatrix}, \quad |2^{(2)}\rangle \equiv \begin{pmatrix} 0 \\ 1 \end{pmatrix} \quad (1.39)$$

for Hamiltonian $\mathbb{H}^{(2)}$ and

$$|1^{(3)}\rangle \equiv \begin{pmatrix} 0 \\ 1 \\ 0 \end{pmatrix}, \quad |2^{(3)}\rangle \equiv \begin{pmatrix} 0 \\ 0 \\ 1 \end{pmatrix} \quad (1.40)$$

for Hamiltonian $\mathbb{H}^{(3)}$.

The probability ρ of finding $|1\rangle$ still in the state $|1\rangle$ varies for different times according to the formula

$$\rho = |\langle 1|e^{-i\mathbb{H}t}|1\rangle|^2. \quad (1.41)$$

In the first case,

$$\rho^{(2)} = \frac{2V^2+\epsilon^2+2V^2\cos\left(t\sqrt{4V^2+\epsilon^2}\right)}{4V^2+\epsilon^2}. \quad (1.42)$$

It is obvious that the frequency is

$$\Omega^{(2)} = \sqrt{4V^2+\epsilon^2}. \quad (1.43)$$

Similarly as above, we can find the probability $\rho^{(3)}$ of finding $|1^{(3)}\rangle$ in the state $|1^{(3)}\rangle$ for the Hamiltonian (1.38):

$$\rho^{(3)} = \frac{\left(\epsilon^2 + V^2 \cos\left(t\sqrt{2V^2+\epsilon^2}\right)\right)^2}{\left(2V^2+\epsilon^2\right)^2}$$
$$= \frac{\left(V^2+\epsilon^2\right)^2}{\left(2V^2+\epsilon^2\right)^2} + \frac{2\left(V^4+V^2\epsilon^2\right)\cos\left(t\sqrt{2V^2+\epsilon^2}\right)}{\left(2V^2+\epsilon^2\right)^2}$$
$$+ \frac{V^4\left(\cos\left(2t\sqrt{2V^2+\epsilon^2}\right)+1\right)}{2\left(2V^2+\epsilon^2\right)^2} \quad (1.44)$$

We can see that we get higher harmonic frequency $\Omega_2^{(3)}$ in addition to the basic frequency $\Omega_1^{(3)}$

$$\Omega_1^{(3)} = \sqrt{2V^2+\epsilon^2}, \quad (1.45a)$$
$$\Omega_2^{(3)} = 2\sqrt{2V^2+\epsilon^2}. \quad (1.45b)$$

2. Computational Methods

Our goal now will be to solve the system of differential equations (1.27). The paramount problem is the integral in (1.27a). We postpone the evaluation of it for a while and turn our attention to orthogonal polynomials, as we will find them very useful later on.

2.1 Orthogonal Polynomials

Let's have $\infty \leq a < b \leq \infty$, a linear vector space $L^2((a,b))$ of square-integrable functions on the interval (a,b) with inner product defined by

$$(f(x), g(x)) = \int_a^b f(x)\overline{g(x)}\mathrm{d}x \tag{2.1}$$

and a set of polynomial functions of degree n $\{f_n(x)\}_{n=0}^{\infty}$ such that

$$\int_a^b f_n(x)\overline{f_m(x)}\mathrm{d}x = \begin{cases} 0 & n \neq m, \\ C_n & n = m, \end{cases} \tag{2.2}$$

where $C_n \in \mathbb{R}$. Then it is said that the set $\{f_n(x)\}_{n=0}^{\infty}$ is orthogonal over interval (a,b). Furthermore, if $C_n = 1$, it's said that the set is orthonormal.

More generally, consider a function $w(x)$, integrable and non-negative on interval (a,b). If $w(x)$ is unbounded on (a,b), than we must require further condition for the moments:

$$\int_a^b x^{\mu} w(x)\mathrm{d}x < \infty, \quad \mu \in \mathbb{N} \tag{2.3}$$

Now we can generalize the previous statement: It's said that the set of polynomials $\{f_n(x)\}_{n=0}^{\infty}$ on a linear vector space $L^2((a,b))$ such that

$$\int_a^b f_n(x)\overline{f_m(x)}w(x)\mathrm{d}x = \begin{cases} 0 & n \neq m, \\ C_n & n = m, \end{cases} \tag{2.4}$$

where $C_n \in \mathbb{R}$, is orthogonal set with respect to the weight function $w(x)$ on (a,b). If $C_n = 1$, then the set is additionally orthonormal.

Many orthogonal and orthonormal polynomials have been found so far. Of our particular interest will be Hermite and Legendre polynomials.

Hermite Orthogonal Polynomials

Hermite orthogonal polynomials appear as a solution of differential equation [4]

$$\frac{\mathrm{d}^2 y(x)}{\mathrm{d}x^2} - 2x\frac{\mathrm{d}y(x)}{\mathrm{d}x} + 2ny = 0, \qquad n = 0, 1, 2, ... \tag{2.5}$$

for $x \in (-\infty, \infty)$ and are orthogonal with respect to the weight function $w = e^{-x^2}$. These polynomials can be also written as:

$$H_n(x) = (-1)^n e^{\frac{x^2}{2}} \frac{\mathrm{d}^n}{\mathrm{d}x^n} e^{-\frac{x^2}{2}} \tag{2.6}$$

Legendre Orthogonal Polynomials

In the same manner, Legendre orthogonal polynomials are solutions of [4]

$$(1-x^2)\frac{\mathrm{d}^2y}{\mathrm{d}x^2} - 2x\frac{\mathrm{d}y}{\mathrm{d}x} + n(n+1)y = 0, \qquad n = 1, 2, ... \tag{2.7}$$

for $x \in (-1, 1)$ with the weight function $w = 1$. They can be written as

$$P_n(x) = \frac{1}{2^n n!}\frac{\mathrm{d}^n}{\mathrm{d}x^n}(x^2-1)^n. \tag{2.8}$$

2.2 Gaussian Quadrature

Our goal is to numerically calculate integral of a given function with a minimum error made. The whole idea of this method is in the Mean value theorem of integral calculus. This theorem states, that there exist a point c in the integration interval such that the definite integral corresponds to the function value at this point multiplied by length of this interval

$$\int_a^b f(x)\mathrm{d}x = (b-a)f(c), \qquad c \in [a, b], \tag{2.9}$$

if $f(c)$ exists.

Gaussian quadrature allows us to rewrite the integral, if we can find n appropriate non-equidistant points $x_i \in \mathbb{R}$ and weights w_i, such that it holds:

$$\int_a^b f(x)\mathrm{d}x = \sum_{i=1}^{n} w_i f(x_i) + K_n(f), \tag{2.10}$$

where $K_n(f) = 0$ if f is a polynomial of degree $\leq 2n-1$ [5].

For a smooth function f which can be well approximated by a polynomial the method is very accurate even for small number of points x_i. All we need is to determine weighs w_i and points x_i, which can be done using the properties of orthogonal polynomials.

It can be shown that orthogonal polynomials of degree n have exactly n distinct roots in the interval (a, b). Moreover, the roots "interleave" the roots of polynomial of degree $n-1$. So there is always one root in between each two adjacent roots of previous polynomial. The most beautiful surprise comes when we find all these roots. They are in fact the points x_i for Gaussian quadrature.

Finding the corresponding weighs w_i is easy in our case as we are about to use either Hermite or Legendre polynomials, which are both well-known sets of functions with known weigh functions. From Gram-Schmidt orthogonalization one can derive formulas for w_i, which will give us all we need for the computation. For Hermite polynomials we get

$$w_i = \frac{2}{(\tilde{H}_n'(x_i))^2}, \tag{2.11}$$

while for Legendre polynomials the weights read

$$w_i = \frac{2}{(1-x_i^2)[P_n'(x_i)]^2}, \tag{2.12}$$

where $\tilde{H}_i$ is normalized Hermite polynomial [6]

$$\tilde{H}_i = \frac{1}{\sqrt{\pi} n! 2^n} H_i. \tag{2.13}$$

These methods are called Gauss-Hermite and Gauss-Legendre quadrature respectively.

Note that in the Gauss-Legendre quadrature we need to transform the integral from interval $(-1, 1)$ to interval (a, b), which can be done by substitution

$$x = \frac{b-a}{2} z + \frac{b+a}{2} \tag{2.14}$$

In the present work, we will use Gaussian quadratures to numerically evaluate the integrals over energy in(1.27).

3. Results and Discussion

3.1 Numerical Approach

As stated in previous chapter, we need to evaluate the integral in the equation (1.27). We do it numerically by Wolfram Mathematica program using Gaussian quadrature, for which we have to choose the appropriate method - either Gauss-Hermite or Gauss-Legendre one.

We want to suppress numerical error to minimum, therefore, we need the continuum to be discretized as finely-grained as possible (regarding time of the computation), that means, we need a polynomial of high order. The higher order we have, the smaller is the error made during computation. The natural choice here is Gauss-Hermite as the integrand V is already in the form of weight function $w = e^{-x^2}$. Moreover, unlike in Gauss-Legendre quadrature, we can precisely evaluate the integral in (1.27) from minus infinity to infinity, whilst using Gauss-Legendre quadrature will force us to restrict ourselves to finite (sufficiently large) interval.

On the other hand, some of the roots of Hermite polynomial are far away form the origin where $V = \alpha e^{-\beta\epsilon^2}$ is effectively zero, therefore, these roots do not really contribute to the resulting sum (2.10). We have to calculate roots of higher order polynomial, if we want higher precision, because the sum (2.10) is mostly dominated by roots near the origin. Legendre polynomials have roots almost uniformly distributed, that means, if we restrict ourselves to finite interval, using the same order of polynomial gives us higher precision.

Another problem comes with calculating weights for Hermite polynomials: The Hermite polynomial in (2.11) becomes in some of the roots far from the origin smaller than the machine precision. As the polynomial appears in the denominator, numerical approach collapses when the order of the polynomial is about 300, while Gauss-Legendre quadrature is still stable even when 1500 equations are given.

Furthermore, the order of the polynomial is equal to the number of equations (1.27a). As the number of equations gets larger, the interval of integration on which the numerical evaluation reasonably simulates the system gets longer (further discussion is in the section 3.3).

For all reasons mentioned above, it was not plausible to use Gauss-Hermite quadrature in the present thesis. We decided to use Gauss-Legendre quadrature, which is already included in Mathematica under the command *GaussianQuadratureWeights* (see Attachment 1). We require the deviation of the numerical integration from the exact solution to be of order 10^{-8} or less, which resulted in the interval $(-55, 55)$. For this interval, converged results were obtained with 1500 integration points. Resulting set of 1501 differential equations (1.27) was solved using the standard Mathematica routine *NDSolve*.

3.2 Exponential Decay According to Perturbation Theory

We numerically compute the probability of finding the initial discrete state $|\Psi(t)\rangle$ still in $|\varphi\rangle$ after a time t (see equation (1.28)) as a function of parameters α and β. For very small β the system is close to Fano model (V is effectively a constant) and the decay is nearly exponential:

$$|\langle\varphi|\Psi(t)\rangle|^2 = |a(t)|^2 \propto e^{-\Gamma t} = e^{-\frac{t}{\tau}} \tag{3.1}$$

The value of the decay constant Γ can be found from first order perturbation theory in the form of Fermi's golden rule, which states:

$$\Gamma = 2\pi|\langle\varphi|\mathbb{H}|E\rangle|^2\delta(E_\varphi - E), \tag{3.2}$$

where $\delta(E_\varphi - E)$ is the Dirac δ-function. Since $E_\varphi = 0$ we get

$$\Gamma = 2\pi|e^{-\beta\epsilon^2}|^2\Big|_{\epsilon=0} = 2\pi|\alpha|^2, \tag{3.3}$$

providing formula for expected decay of $|\varphi\rangle$ into the quasi-continuum

$$|a(t)|^2 = e^{-2\pi|\alpha|^2 t}. \tag{3.4}$$

3.3 Numerically Simulated Decay

We start examination of the time evolution with some technical aspects. Figure 3.1 shows numerically calculated probability (1.28) (blue curve, denoted by n.c.) compared with the exponential decay predicted by (3.4) (yellow curve). It reveals slight abnormality in exponential decay. As a residue of numerical discretization of the continuum, by which we effectively "enclosed" the system into a box finite in space, the wave function reflect from the wall of the well. We will restrict ourselves to a smaller interval of time, as this reflection is not of any physical meaning to us. The results can be considered valid only for times < 50 for used numerical parameters (mainly the degree of Legendre polynomial in Gauß quadrature set to 1500).

Another anomaly, seen in Figure 3.2, are "echoes" in exponential decay. For $\alpha = 1/5$, $\beta = 20$ we are far away from Fano model. Parts of the continuum near origin are strongly coupled to the discrete state compared to more distant parts, giving rise to more complicated phenomena in the time evolution. We can also see that the second echo mix together with the reflection.

We start the examination with Figure 3.3, where we are close to Fano model at the beginning, and as β increases, we are leaving the area where Fano model is still valid. We can see that the expected curve (3.4) starts to deviate significantly around $\beta = 1$ from numerically calculated $|a(t, \alpha, \beta)|^2$. Around $\beta = 10$ the first oscillations of probability appear with a frequency around 25 time units. This frequency decreases with β and for $\beta = 140$ (Figure 3.3(h)) the oscillations disappear, as the frequency is longer than the interval of simulation (1.28).

In Figure 3.4 we can see the oscillations playing the main role. As $\alpha = 2$ the discrete state is now coupled to the continuum so strongly that the system

partially reflects back to the discrete state $|\varphi\rangle$ before it can escape to infinity. The rest of it goes away into the continuum. That explains oscillations of the probability with exponential decline. We can see that the exponential decline is slower with β increasing.

We obviously can not talk here about Fano model any more, yet the only parameter that has changed is α. But Fano model places no restrictions on how strong the coupling should be. It only requires the coupling to be constant, which is ensured by small β. Therefore, according to Fano, the parameter α should not be very important, but still we see that large α causes oscillations even for those values of β for which the system decays exponentially in the case of smaller α (Figure 3.3).

Whether the oscillations appear or not evidently depends on chosen value of α and β, with α as the dominant variable. It can be seen clearly in Figure 3.5 that different α can entirely switch the regime between exponential decay and oscillatory mode. Moreover, when the oscillations first show up (Figure 3.5(f)) the frequency of them corresponds to the point where expected probability (3.4) of finding $|\Psi(t)\rangle$ in $|\varphi\rangle$ effectively reaches zero, which supports our theory - first, the decay follows to expected behaviour of Fano model, but strong coupling forces part of the system to return to the discrete state. When we continue with larger and larger α, the initial decay will be slower than expected and the frequency slightly decreases.

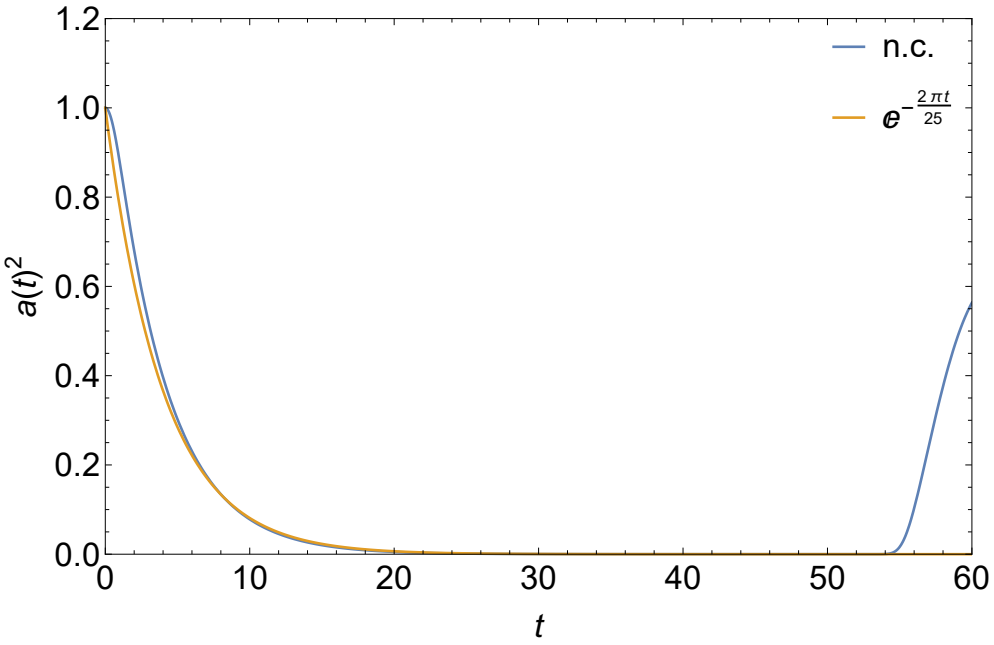

Figure 3.1: Decay of the discrete state $|\varphi\rangle$ into the continuum of states $|E\rangle$. The blue curve, denoted by n.c., shows numerically calculated probability according to Equation (1.28). The predicted decay (Equation (3.4)) is the yellow curve. The paremeters are set $\alpha = 1/5$, $\beta = 1/5$.

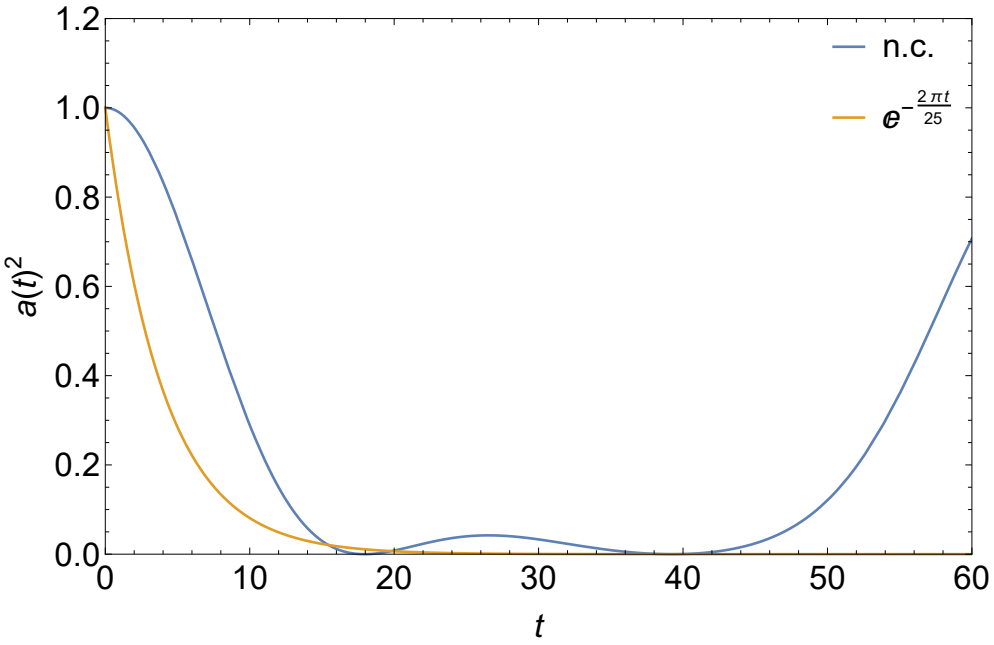

Figure 3.2: Decay of the discrete state $|\varphi\rangle$ into the continuum of states $|E\rangle$. The color coding is the same as in Figure 3.1. The paremeters are set $\alpha = 1/5$, $\beta = 20$.

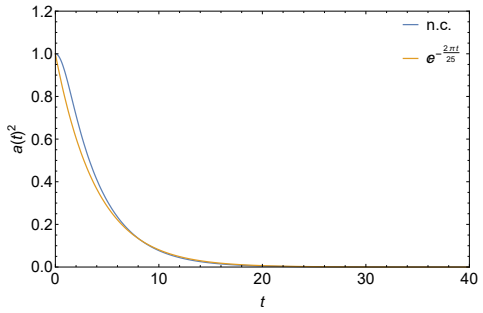

(a) $\beta = 1/5$

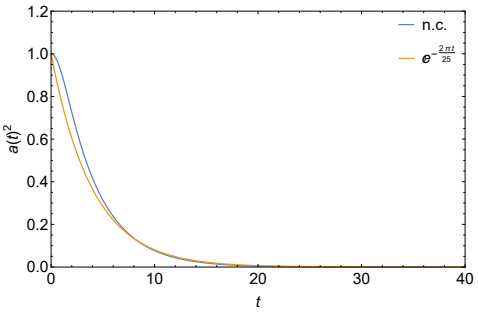

(b) $\beta = 1/4$

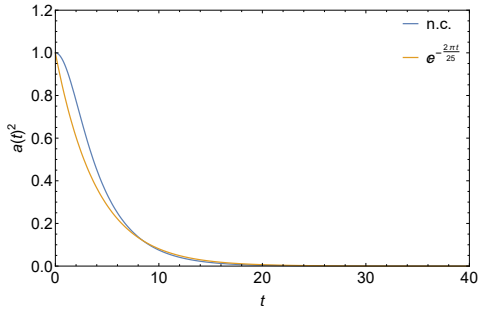

(c) $\beta = 1/2$

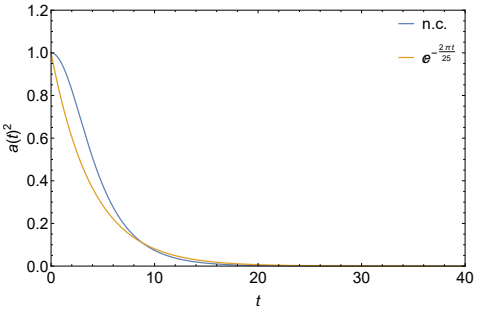

(d) $\beta = 1$

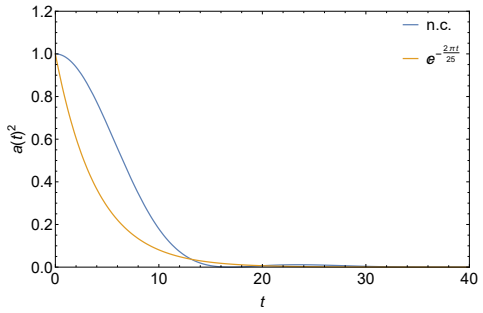

(e) $\beta = 10$

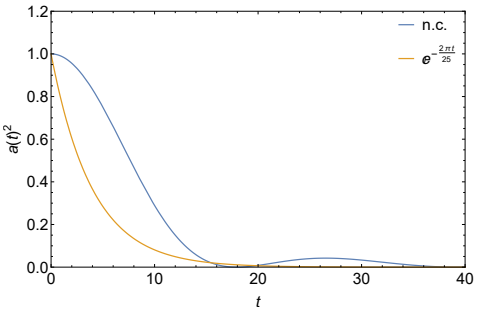

(f) $\beta = 20$

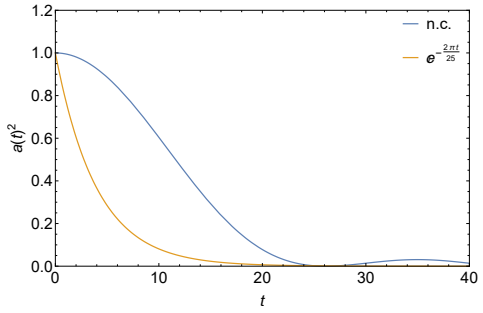

(g) $\beta = 100$

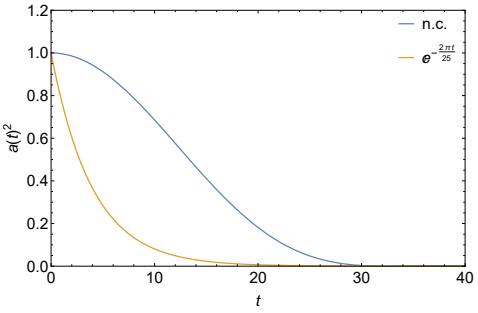

(h) $\beta = 140$

Figure 3.3: The decay of the discrete state $|\varphi\rangle$ into the continuum of states $|E\rangle$. The blue curve, denoted by n.c., shows numerically calculated probability according to Equation (1.28). The predicted decay (Equation (3.4)) is the yellow curve. The paremeter is set $\alpha = 1/5$, β varies.

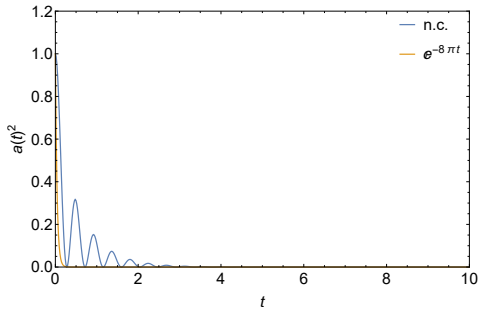

(a) $\beta = 1/50$

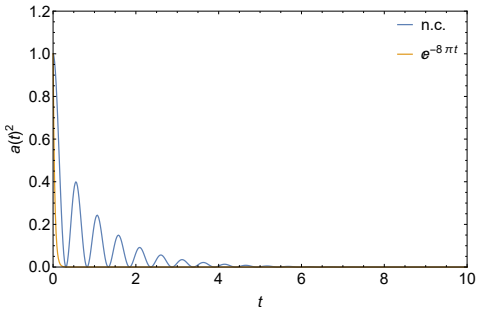

(b) $\beta = 1/30$

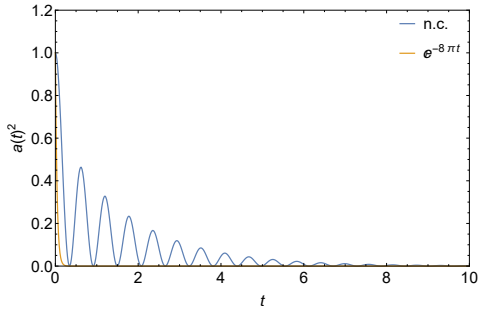

(c) $\beta = 1/20$

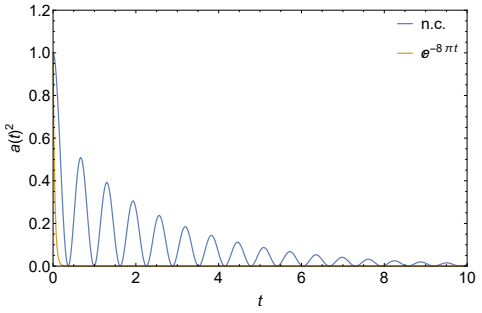

(d) $\beta = 1/15$

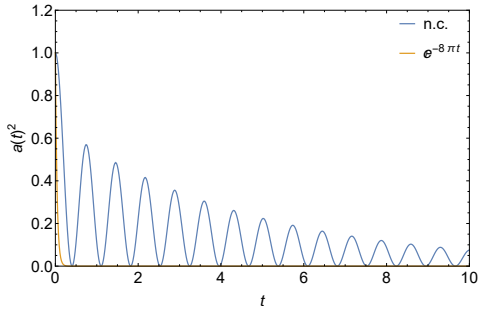

(e) $\beta = 1/10$

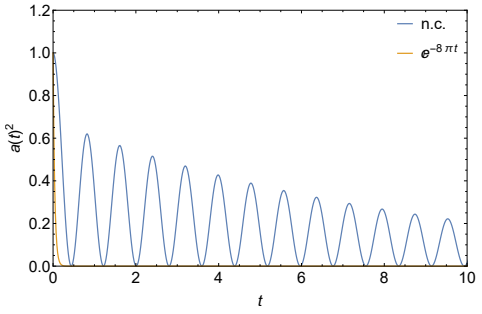

(f) $\beta = 1/7$

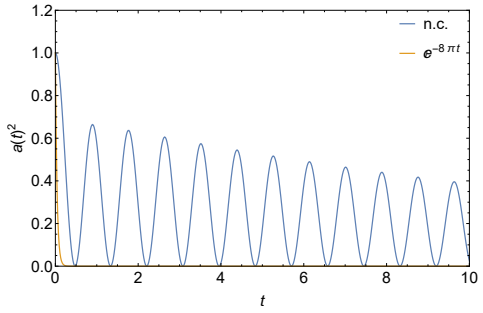

(g) $\beta = 1/5$

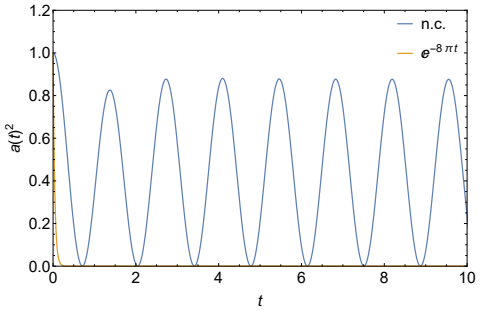

(h) $\beta = 1$

Figure 3.4: The decay of the discrete state $|\varphi\rangle$ into the continuum of states $|E\rangle$. The blue curve, denoted by n.c., shows numerically calculated probability according to Equation (1.28). The predicted decay (Equation (3.4)) is the yellow curve. The paremeter is set $\alpha = 2$, β varies.

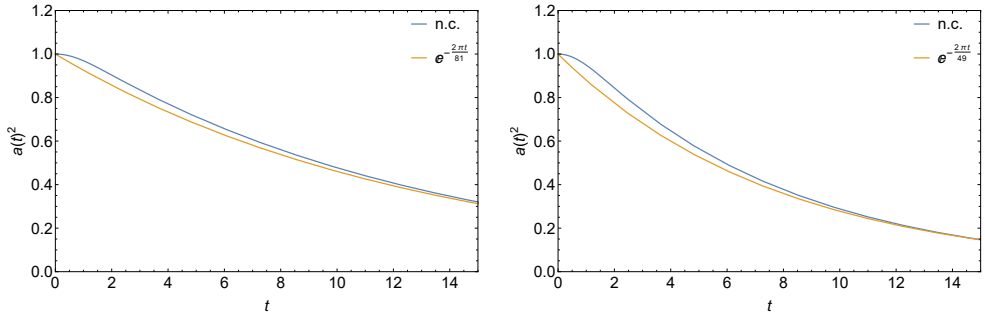

(a) $\alpha = 1/9$

(b) $\alpha = 1/7$

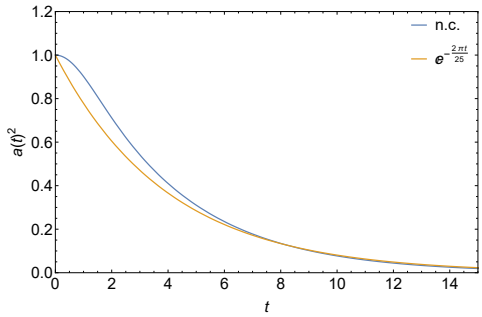

(c) $\alpha = 1/5$

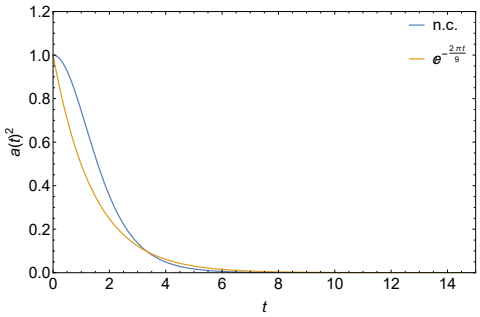

(d) $\alpha = 1/3$

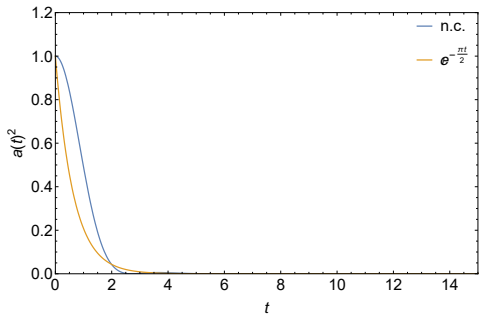

(e) $\alpha = 1/2$

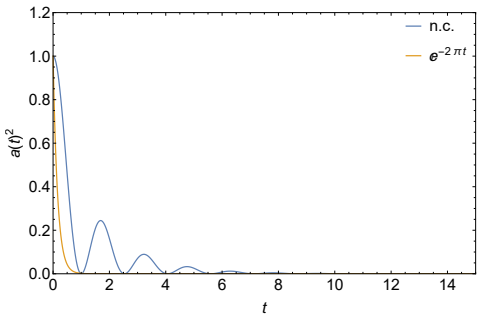

(f) $\alpha = 1$

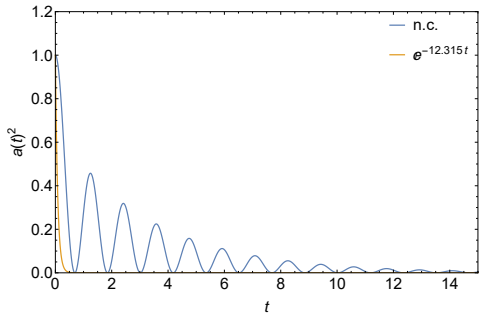

(g) $\alpha = 1.4$

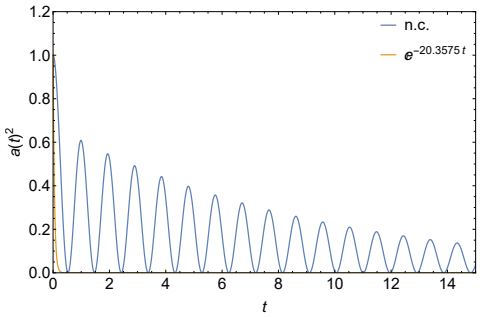

(h) $\alpha = 1.8$

Figure 3.5: The decay of the discrete state $|\varphi\rangle$ into the continuum of states $|E\rangle$. The blue curve, denoted by n.c., shows numerically calculated probability according to Equation (1.28). The predicted decay (Equation (3.4)) is the yellow curve. The paremeter is set $\beta = 1/5$, α varies.

3.3.1 System in the Non-Oscillatory Mode

In this short section, we would like to verify correctness of our model by the limit when the coupling (1.23) tends to a constant one. We expect the decay of the system will be approaching the exponential decay predicted by Fano model, which will prove consistence of our theory.

Having the resulting function $|a(t, \alpha, \beta)|^2$ numerically calculated, we fit it by

$$f(t) = ce^{-\frac{t}{\tilde{\tau}}} \tag{3.5}$$

with $c, \tilde{\tau}$ as fitting parameters. We expect values $\tau = \Gamma^{-1}$ (see equation (3.1)), when we are in non-oscillatory mode. For different α and β the resulting values $\tilde{\tau}$ are in Tables 3.1, 3.2, and 3.3. As we can see, relative errors of $\tilde{\tau}$ vary from tens of percent when α and β are larger than approximately 1/4, to effectively zero for very small α and β, when we are close to Fano model and (3.4) is valid.

Table 3.1 shows results for quite large α and β for which the relative errors of $\tilde{\tau}$ go up to 40% and never under 5%. As stated before, α is the dominant parameter causing deviation from exponential decay. As we can see in Table 3.2, small α may suppress relative errors even for not really small β. For both parameters far under the value of 1/4, the relative error is negligible (Table 3.3).

β	$\tilde{\tau}$	Relative error
10.0	5.62	0.41
5.00	4.88	0.23
1.00	3.89	0.02
0.50	3.74	0.06
0.33	3.71	0.07
0.25	3.70	0.07
0.20	3.70	0.07
0.17	3.71	0.07
0.14	3.72	0.07
0.13	3.73	0.06
0.11	3.74	0.06

Table 3.1: Table of fitted parameter $\tilde{\tau}$ from Equation (3.5). The parameter is set $\alpha = 1/5$, β varies. Assumption $\tau = \Gamma^{-1}$ yields (see Equation (3.3)) $\tau = 3.98$. Relative error is given by $\frac{|\tilde{\tau}-\tau|}{\tau}$.

α	τ	$\tilde{\tau}$	Relative error
0.33	1.43	1.25	0.12
0.25	2.55	2.31	0.09
0.20	3.98	3.70	0.07
0.17	5.73	5.44	0.05
0.14	7.80	7.50	0.04
0.13	10.19	9.88	0.03
0.11	12.89	12.59	0.02
0.10	15.92	15.62	0.02
0.07	35.81	35.58	0.01
0.05	63.66	63.60	0.00

Table 3.2: Table of fitted parameter $\tilde{\tau}$ from Equation (3.5). The parameter is set $\beta = 1/5$, α varies, $\tau = (2\pi|\alpha|^2)^{-1}$. Relative error is given by $\frac{|\tilde{\tau}-\tau|}{\tau}$.

α	τ	$\tilde{\tau}$	Relative error
0.20	3.99	3.95	0.0081
0.17	5.73	5.71	0.0039
0.14	7.80	7.78	0.0021
0.13	10.19	10.17	0.0013
0.11	12.90	12.88	0.0008
0.10	15.92	15.91	0.0006
0.07	35.81	35.80	0.0002
0.05	63.66	63.66	0.0001
0.02	397.89	397.88	0.0000
0.01	1591.55	1591.54	0.0000

Table 3.3: Table of fitted parameter $\tilde{\tau}$ from Equation (3.5). The parameters are set $\beta = \alpha^4$, $\tau = (2\pi|\alpha|^2)^{-1}$. Relative error is given by $\frac{|\tilde{\tau}-\tau|}{\tau}$.

3.3.2 System in the Oscillatory Mode

In general, oscillations appear in multi-level systems, therefore these systems will be of our particular concern. We shall try to describe our discretized continuum as a multi-level system, starting with two and three level systems. We remind here results from Section 1.3 – the frequencies for two level system $\Omega^{(2)}$ and three level system $\Omega^{(3)}$ read

$$\Omega^{(2)} = \sqrt{4V^2 + \epsilon^2} \tag{3.6a}$$

$$\Omega_1^{(3)} = \sqrt{2V^2 + \epsilon^2} \tag{3.6b}$$

$$\Omega_2^{(3)} = 2\sqrt{2V^2 + \epsilon^2} \tag{3.6c}$$

In oscillatory mode, we can find frequency ω of oscillations as a function of "full width at half maximum" ($FWHM$) of the coupling $V(\alpha, \beta, \epsilon)$. We approximate $\epsilon \cong FWHM$ as it represents characteristic energetic distance between discrete state $|\varphi\rangle$ and the states of the continuum.

We set $\alpha = 2$ as it provides clear probability oscillations for various β. We can see (Table 3.4) that frequency ω of oscillations decreases with decreasing $FWHM$. Obviously we cannot compare generalized Fano model with two level system: As $FWHM$ tends to zero (β increasing), the term $4V^2$ tends to 4 and equation (3.6a) gives $\sqrt{4} = 2$. The same problem arises with the three level system, only equation (3.6b) gives $\sqrt{2}$. But frequency of oscillations ω decreases far more, tending to zero. Therefore, neither the two level system nor the three level system describes the observed frequency correctly. In fact, ω as function a of α and β seems to be accurately fitted by $\sqrt{FWHM}$ – see Figure 3.6. As the continuum is now due to the discretization effectively multi-level system, we may try to simulate it by such a system. We modify equations (1.27) for multi-level system of energies E_i. That is, we replace the integral in (1.27a) by sum, leaving out the weights. We get a set of differential equations

$$i\frac{\mathrm{d}a(t)}{\mathrm{d}t} = \sum_{i=1}^{\infty} b(t, E_i)V(E_i), \tag{3.7a}$$

$$i\frac{\mathrm{d}b(t, E_i)}{\mathrm{d}t} = a(t)V^*(E_i) + b(t, E_i)E_i, \tag{3.7b}$$

As we used Gauss-Legendre quadrature to numerically evaluate coefficients $a(t)$ and $b(t, E)$ above, we now effectively just set all weights equal to one. When evaluating (1.27), the weights were in range of approximately $0.02 - 0.9$, so we enlarge all of them. The coupling therefore appears stronger to the system, giving rise to oscillations even for such α, β the system used to decay exponentially (see Figure 3.7) and accentuates the oscillation when the generalized Fano model oscillates (Figure 3.8). Also, when evaluating (1.27), we used for discretization roots of Legendre polynomials, which are almost uniformly distributed. For (3.7) we discretize the continuum uniformly to 1500 levels.

The number of levels in multi-level system is closely linked up with the frequency of the oscillations. On the other hand, for the generalized Fano model with continuum of the final states, the resulting numerically simulated time evolution for system with $|\Psi(t)\rangle$ evaluated from Equation (1.27) is stable and the

change in the frequency of the oscillations when 1500 or 300 differential equations (1.27a) is of order 10^{-2}. This confirms that the numerical approach to treat the continuum is correct.

Even though multi-level system appears to behave completely differently, it may qualitatively describe our system. Compare the green curve in Figure 3.7, denoted by n.c.a and representing numerically calculated probability according to Equation (1.28), where $|\Psi\rangle$ is numerically evaluated from (3.7), with the blue curve in Figure 3.5(f). Similarly, the green curve in Figure 3.8, denoted by n.c. a, representing the same system, behaves alike the blue curve in Figure 3.4(h). The only change is in the frequency of the oscillations which is, as already mentioned, a function of number of the energy levels in the multi-level system.

From Table 3.4, it can be seen that the limit of the frequency $\Omega^{(n)}$ decreases for large β for n-level system. We can expect that with β and n tending to infinity (i.e., continuum of states with very narrow coupling), the frequency of the oscillation tends to zero. The same behaviour has the system with $|\Psi(t)\rangle$ evaluated from Equation (1.27) using Gaussian quadrature.

Besides, from each energy level, new higher harmonic frequency appears (similarly as in (3.6)). When we put them together, they provides oscillations, if α is sufficiently small, with exponential decrease (Figure 3.7). For α large enough, the exponential decrease becomes negligible on the interval of evaluating time evolution (Figure 3.8).

β	FWHM	ω	$\Omega^{(2)}$	$\Omega^{(3)}$
0.005	23.55	3.30	11.94	11.86
0.01	16.65	2.71	8.56	8.44
0.02	11.77	2.28	6.22	6.05
0.03	9.12	1.94	4.98	4.77
0.05	7.45	1.72	4.23	3.98
0.07	6.45	1.58	3.79	3.52
0.10	5.27	1.40	3.31	2.99
0.11	5.00	1.36	3.20	2.87
0.13	4.71	1.31	3.09	2.75
0.14	4.41	1.26	2.98	2.62
0.17	4.08	1.21	2.86	2.48
0.20	3.72	1.14	2.73	2.34
1.00	1.67	0.73	2.17	1.64
1.2	1.52	0.70	2.14	1.61
1.5	1.36	0.66	2.11	1.57
1.7	1.28	0.64	2.10	1.55
2	1.18	0.61	2.08	1.53
2.2	1.12	0.60	2.08	1.52
2.5	1.05	0.58	2.07	1.51
3	0.96	0.55	2.06	1.49
4	0.83	0.51	2.04	1.47
5	0.74	0.48	2.03	1.46
7	0.63	0.44	2.02	1.45
10	0.53	0.40	2.02	1.44
15	0.43	0.36	2.01	1.43
20	0.37	0.34	2.01	1.43
50	0.24	0.27	2.00	1.42
75	0.19	0.24	2.00	1.42
100	0.17	0.22	2.00	1.42
500	0.07	0.06	2.00	1.41

Table 3.4: Table of parameter ω - frequency of oscillations. The parameter is set $\alpha = 2$, β varies. Frequencies $\Omega^{(2)}$ and $\Omega^{(3)}$ are given by equations (3.6a) and (3.6b).

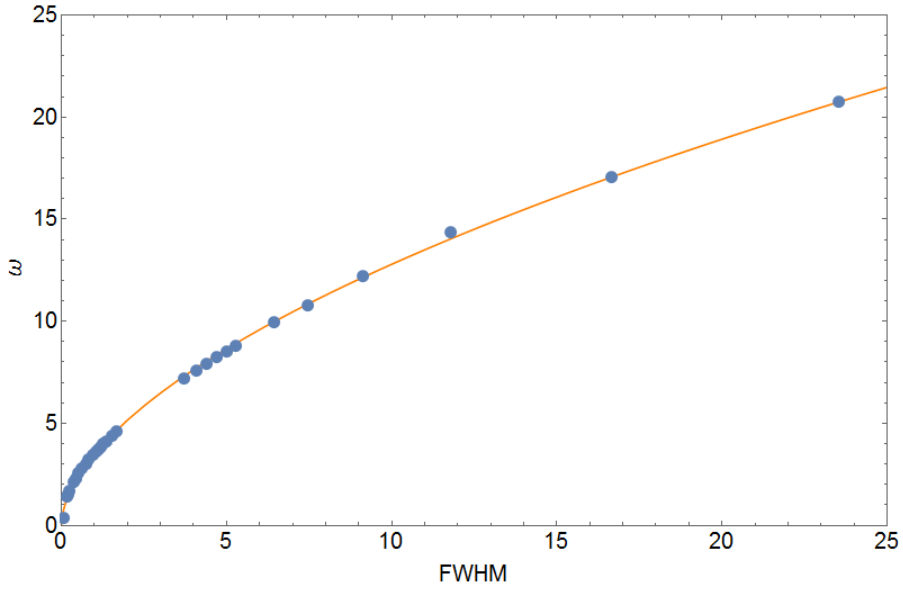

Figure 3.6: The dependence of frequency of oscillations ω on $FWHM$ of the coupling (1.23). Blue points are taken from Table 3.4, yellow curve is the fitted function $f(FWHM) = 3.48(FWHM)^{0.56}$.

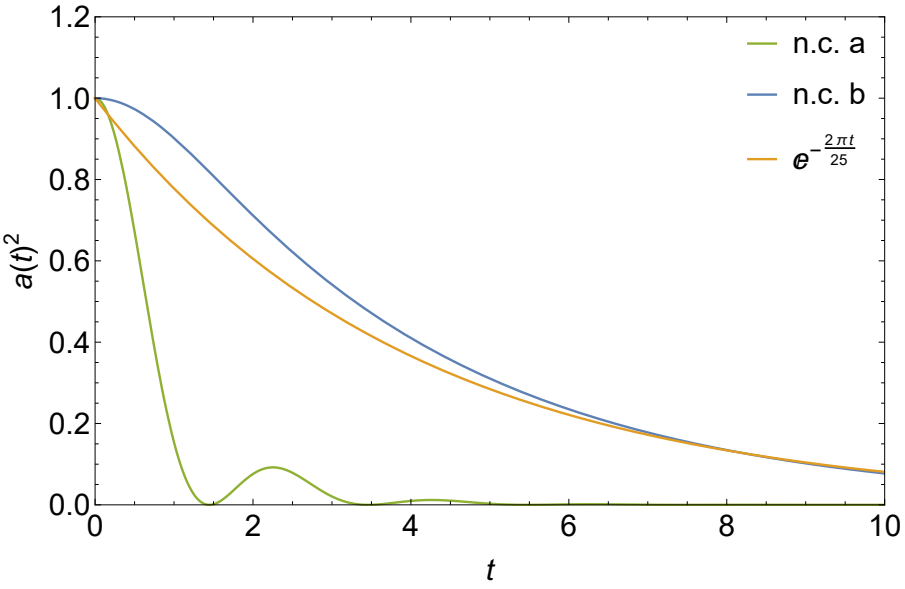

Figure 3.7: The decay of $|\varphi\rangle$ into a system of 1500 states $|E_i\rangle$ uniformly distributed over interval (-55,55). The green curve, denoted by n.c. a, shows numerically calculated probability according to Equation (1.28), where $|\Psi\rangle$ is numerically evaluated from (3.7). The blue curve, denoted by n.c. b, shows numerically calculated probability according to Equation (1.28), where $|\Psi\rangle$ is numerically evaluated from (1.27). The predicted decay (Equation (3.4)) is the yellow curve. The parameters are set $\alpha = 1/5$, $\beta = 1/5$.

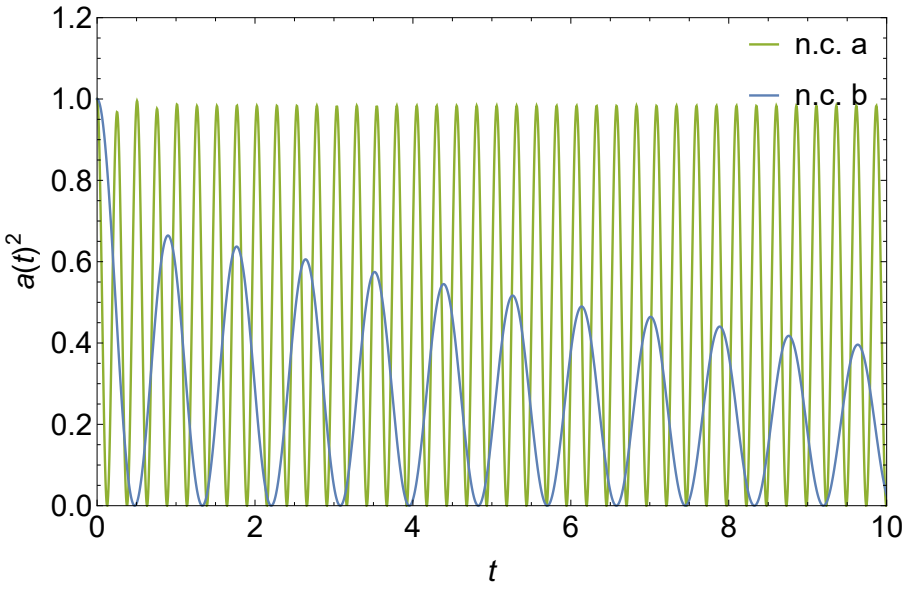

Figure 3.8: The decay of $|\varphi\rangle$ into a system of 1500 states $|E_i\rangle$ uniformly distributed over interval (-55,55). The green curve, denoted by n.c. a, shows numerically calculated probability according to Equation (1.28), where $|\Psi\rangle$ is numerically evaluated from (3.7). The blue curve, denoted by n.c. b, shows numerically calculated probability according to Equation (1.28), where $|\Psi\rangle$ is numerically evaluated from (1.27). The parameters are set $\alpha = 2$, $\beta = 1/5$.

3.3.3 Transition between the Oscillatory and the Non-Oscillatory Mode

In this section, we would like to find criteria by which we can determine whether the oscillations appear or not. We have seen already that it depends on the parameters α and β in the coupling (1.23). In particular, on the magnitude of the coupling, given by

$$\|V\| = \left(\int_{-\infty}^{\infty} |V(E)|^2 \mathrm{d}E\right)^{1/2} \propto \frac{\alpha}{\sqrt[4]{\beta}}. \tag{3.8}$$

We anticipate that transition from non-oscillatory to oscillatory mode is closely linked to the magnitude of V, more precisely, to its specific value. We may try to find a dimensionless expression, which will predict whether the oscillations appear or not, such as

$$\frac{\alpha}{FWHM} \propto \alpha\sqrt{\beta}. \tag{3.9}$$

However, it turns out that the formula

$$\frac{\alpha}{\sqrt{FWHM}} \propto \alpha\sqrt[4]{\beta} \tag{3.10}$$

is better quantity even though it is not dimensionless. This choice has two motives: First, the term $\sqrt[4]{\beta} \propto 1/\sqrt{FWHM}$ appears in equation (3.8); second, we have seen in previous section that frequency of oscillations ω behaves as $\sqrt{FWHM}$.

We now briefly elaborate the dimensional analysis of our problem. We see that for β holds

$$\left[\sqrt[4]{\beta}\right] = E^{-\frac{1}{2}} = \lambda, \tag{3.11}$$

where E is a unit of energy and λ is a unit of wavelength (of a particle representing our system). For α we have

$$[\alpha] = E = V, \tag{3.12}$$

where V is a unit of strength of the coupling. Summing it all up, we get

$$\left[\alpha\sqrt[4]{\beta}\right] = V\lambda = K \tag{3.13}$$

where K is a specific constant, corresponding to the transition from exponential decay regime to the oscillatory mode.

The obtained result can be understood quite straightforwardly: For a strong coupling (in some sense), the particle needs to be fast enough to escape to infinity before it is captured back to the discrete state, which corresponds to a short wavelength. And the other way around - when the coupling is weak, for the particle it is easy to escape even with small amount of energy (long wavelength).

For $\alpha\sqrt[4]{\beta} > K$, either the coupling is too strong or the particle does not possesses enough energy to escape. In both cases, the oscillations of probability appear. When $\alpha\sqrt[4]{\beta} < K$, the coupling is too weak (or the particle is too fast) to capture the particle back to the discrete state before it escapes to infinity, so it leaves the discrete state and we observe simple exponential decay. This is in conformity with the observed behaviour (see Figure 3.5). We have seen in the section 3.3.2 that α is the dominant parameter switching the regimes, which make

perfect sense, as $\alpha\sqrt[4]{\beta}$ is much more slowly increasing function of β in comparison with its strong dependence on α.

The Table 3.5 shows several values of α and β for which the oscillations first appear. These values are only approximate, because the precise point of appearance of the oscillations is rather subjective. Yet the quantity $\alpha\sqrt[4]{\beta}$ stays constant satisfactorily, confirming our analysis and determining K to be approximately $K \cong 0.32$.

α	β	$\alpha\sqrt[4]{\beta}$
5,00	$1,7.10^{-5}$	0,32
1,00	0,01	0,32
0,90	0,02	0,32
0,80	0,02	0,32
0,75	0,03	0,32
0,50	0,15	0,31
0,25	2,60	0,32

Table 3.5: Table of approximate parameters α and β, for which oscillations appear for the first time.

Conclusion

In the beginning of this thesis, Fano description of a discrete state coupled to a continuum of states by a coupling independent of the energy of the continuum is introduced. Generalized version of Fano model for time-dependent coupling is then outlined, followed by a brief elaboration on special systems of two and three energy levels. Finally, needful theory of numerical computation is presented.

In the second part of this thesis, obtained results are summarized. The time evolution of the system was numerically simulated (using Gauss quadrature, Legendre polynomials, and numerical solution of a set of differential equations), in particular the probability of finding the system in its initial state. It turnes out that the probability for some forms of the coupling exponentially decays and for some of them oscillates with much slower exponential decrease.

The non-oscillatory mode appears when coupling is close to a constant one, that means when Fano model becomes a good approximation. The predictions of first order perturbation theory then correspond to system's time-evolution.

The oscillations appear when coupling is no longer satisfactorily constant. The frequency of oscillations behaves as a square root of $FWHM$ of the coupling, tending to zero with $FWHM$ tending to zero. The frequency is compared with two and three level system, neither of which depicts the system precisely enough. The multi-level system is then discussed and its qualitative behaviour seems to characterise generalized Fano model quite well.

In the last subsection the transition point between both modes is discussed. The quantity that determines the time evolution mode (exponential or oscillatory) is found and its specific value corresponding to the transition from one regime to the other is determined. Furthermore, explanation of its physical meaning is given.

Bibliography

[1] Grynberg Cohen-Tannoudji, Dupon-Roc. *Atom-Photon Interaction*. John Wiley and Sons, Inc., 1998.

[2] Laloe Cohen-Tanouji, Diu. *Quantum Mechanics*, volume 2. John Wiley and Sons, 2005.

[3] Laloe Cohen-Tanouji, Diu. *Quantum Mechanics*, volume 1. John Wiley and Sons, 2005.

[4] Stocker W. Harris. *Handbook of Mathematics and Computational Science*. Springer, New York, 1998.

[5] Horst Stocker John W. Harris. *Handbook of Mathematics and Computational Science*. Springer, New York, 1998.

[6] Press at al. *Numerical Rrecipes*. second edition. Cambridge University Press, 1992.

Attachment

Attachment 1 - Programme

α = ; β = ;
fitdolni = 0.7;
fithorni = 50;
resdolni = 0;
reshorni = 60;
pocet = 5000;
krok = (fithorni - fitdolni)/pocet;
Nq = 1500 ;
frekvence = ;
<< NumericalDifferentialEquationAnalysis
V = Function[e, Exp[-$e^2\beta$] α] ;
GQ = GaussianQuadratureWeights[Nq, -55, 55, 32]];
bs = Table[b[i][t], { i, 1, Nq + 1}];
coupling = Sum[GQ[[i]][[2]]*bs[[i]]*V[GQ[[i]][[1]]], { i, 1, Nq}];
Eq1 = { I D[bs[[Nq + 1]], t] == coupling};
Eq2 = Table[I D[bs[[i]], t] == GQ[[i]][[1]]*bs[[i]] + bs[[Nq + 1]]*V[GQ[[i]][[1]]],
{ i, 1, Nq}];
Eq3 = {(bs[[Nq + 1]] /. t -¿ 0) == 1.0} ;
Eq4 = Table[(bs[[i]] /. t -¿ 0) == 0.0, { i, 1, Nq}];
Eq = Join[Eq1, Eq2];
Eq = Join[Eq, Eq3];
Eq = Join[Eq, Eq4];
sol = NDSolve[Eq, bs, { t, resdolni, reshorni}];
chci = Function[t, Re[bs[[Nq + 1]]*Conjugate[bs[[Nq + 1]]] /. sol[[1]]]];
fitdata = Table[{ N[t], chci[t]}, { t, fitdolni, fithorni, krok}]];
fit = NonlinearModelFit[fitdata, a (Cos[frekvence*t*2 π] + 1)
Exp[-t/τ], { a, b, c, τ}, t];
τ = fit["ParameterTable"][[1]][[1]][[5]][[2]];
relativnichybatau = fit["ParameterTable"][[1]][[1]][[5]][[3]]/
fit["ParameterTable"][[1]][[1]][[5]][[2]]
χ = fit["ANOVATableSumsOfSquares"][[1]]/pocet
ft = Normal[fit];
Plot[{ ft, bs[[Nq + 1]]*Conjugate[bs[[Nq + 1]]] /. sol }, { t, resdolni, reshorni}]